Research Article

Investigation of Endoplasmic Reticulum Stress and Apoptosis Caused by Malachite Green-Mediated Sonodynamic Therapy in HL60 Cells

Metin Caliskan[1], Sercin Ozlem Caliskan[2], Gulsen Bayrak[3]

[1]Uşak University, Faculty of Medicine, Department of Medical Biology, Uşak, Türkiye
[2]Uşak University, Faculty of Medicine, Department of Biophysics, Uşak, Türkiye
[3]Uşak University, Faculty of Medicine, Department of Histology and Embryology, Uşak, Türkiye

Abstract

Aim: Sonodynamic antitumor therapy is a promising, novel method for the treatment of cancer. To determine the effects of malachite green (MG) in the presence of ultrasound (US), MG was tested in vitro on HL60 cells at different concentrations as a sonodynamic compound. We investigated cell viability, morphology, and the occurrence of endoplasmic reticulum (ER) stress after MG-mediated sonodynamic therapy (SDT) in HL60 cells.

Material and Method: Four groups were formed, including a control group, a group subjected to ultrasound (US) only, a group treated with various concentrations of MG, and a group treated with US using the same concentrations. The cells were treated with 1MHz ultrasound at 2 W/cm^2 for 3 minutes. The assessment of cell viability was conducted 24 hours post-treatment through the utilization of the 3-(4,5-dimethylthiazol-2-yl)-2,5-diphenyl tetrazolium bromide (MTT) assay. Cell morphology and apoptotic index were determined using Giemsa staining, while GRP78 and PERK expressions were determined through immunocytochemistry staining.

Results: The cell cytotoxicity of HL60 cells significantly increased after MG-mediated sonodynamic therapy. After treatment, apoptotic cells with micronuclei were observed morphologically. Significant levels of GRP78 and PERK expression were observed in all groups, except for PERK expression in the US group, compared to the control group.

Conclusion: The induction of ER stress, accompanied by intense apoptosis and a marked decrease in cell viability, demonstrates the potential of MG-mediated sonodynamic therapy in cancer treatment. Investigating ER stress as a molecular target may contribute to improving the treatment method.

Keywords: HL60 cells, malachite green, sonodynamic therapy, apoptosis, ER stress

INTRODUCTION

Surgery, radiotherapy, and chemotherapy are classic treatment methods for cancer. Targeted therapy, hormonal therapy, and immunotherapy are alternative methods reported in cancer treatment. Even though these treatments had clinical success, they also have side effects and disadvantages. Chemotherapeutic drugs may cause side effects such as liver damage, gastrointestinal toxicity, and immunosuppression, while radiotherapy may have toxic effects on normal tissue. Surgical procedures may cause trauma and tumor metastasis. Therefore, non-invasive, effective, non-toxic, and reproducible cancer treatment methods are necessary (1,2).

Photodynamic therapy (PDT) has been utilized as a non-toxic and non-invasive method for tumor treatment in recent years. The mechanism of action of PDT is based on the activation of a photosensitizer that selectively accumulates in tumor tissue when exposed to light of an appropriate wavelength. This activation initiates a series of biochemical events that can potentially cause damage and lead to the death of the target tissue (3). Numerous studies have shown that PDT is an effective alternative treatment method for various cancers. Nevertheless, its effectiveness in the treatment of deep tumors is limited due to the shallow depth of penetration of light (4).

Sonodynamic therapy (SDT) emerged after Yumita and Umemura discovered in 1989 that hematoporphyrin, a photosensitizer, could be activated by ultrasound (US) and kill tumor cells (5). SDT refers to the process in which a sonosensitizer is activated by US, resulting in the production of reactive oxygen species (ROS) (6-9). The mechanism of SDT remains unclear. The mechanisms reported in the literature are the ultrasound-induced cavitation effect and the ROS formation. The predominant mechanism widely acknowledged involves the generation of ROS induced by pyrolysis or sonoluminescence. Ultrasound is a mechanical wave that has many advantages, including high-level concentrated energy, directability, and long-distance propagation. SDT has significant potential in the treatment of deep-seated tumors due to its ability to penetrate deep tissues and cause minimal damage to surrounding normal tissues (10,11).

The endoplasmic reticulum (ER) is a central organelle that is primarily responsible for protein synthesis, folding, and modification, and it controls various cellular functions, including intracellular Ca^{2+} balance and maintenance of cellular homeostasis (12). Sonodynamic treatment causes abundant ROS production, which leads to an increase in ER stress and the induction of apoptosis if this stress cannot be tolerated (13,14). The accumulation of misfolded proteins in the ER after sonodynamic treatment leads to the induction of Glucose-regulated protein 78 (GRP78), which acts as a chaperone and master regulator of the Unfolded Protein Response (UPR) (15). PERK is a transmembrane protein localized in ER. Under normal conditions, PERK is inactive and is complexed with ER chaperone immunoglobulin binding proteins. The complex is disrupted when ER stress occurs, and PERK inactivates eIF2, which is required for protein synthesis, by phosphorylating it, thereby suppressing translation and reducing ER stress (16).

The effectiveness of sonodynamic therapy largely depends on the efficacy of the sonosensitizer. Malachite green (MG) is a cationic dye with a triphenylmethane structure derived from dimethyl aniline and benzaldehyde (17). Due to the structural properties of triacyl methane dyes, their selective localization ability attracts attention as antimicrobial and anticancer agents (18). The literature lacks studies on the efficacy of sonodynamic treatment using MG, which stands out as a photosensitizer. The present study investigated the effects of MG-mediated SDT on cell viability, morphology, apoptosis, and ER stress in HL60 acute promyelocytic leukemia cells.

MATERIAL AND METHOD

HL60 Cell Culture

The human acute promyelocytic leukemia cell line HL60 was cultured in RPMI 1640 with L-glutamine medium (CEGROGEN, Biotech, Germany), supplemented with 10% fetal bovine serum, 100 U/mL penicillin, and 100 µg/mL streptomycin (Sigma, St. Louis, MO, USA).

Preparation of Stock Solutions of Malachite Green

MG stock solution (Sigma-Aldrich, USA) was prepared in PBS at a concentration of 50 µM. MG dilutions of 3.12, 1.56, 0.78, 0.39, 0.19, and 0.09 µM were prepared from the stock MB solution using RPMI 1640 medium. An equal amount of fresh medium containing 1×10^5 cells was added to the prepared dilutions.

Experimental Groups

Group 1: (Control) The control group is composed of control untreated cells.

Group 2: (US) Only ultrasound was performed on the cells at a frequency of 1 MHz with an intensity of 2 W/cm² and a distance of 2 cm for 3 minutes

Group 3: (MG) Cells were exposed to MG at doses of 3.12, 1.56, 0.78, 0.39, 0.19, and 0.09 µM for one hour at 37°C, then the free MG was removed.

Group 4: (MG+SDT) Cells were incubated with MG doses of 3.12, 1.56, 0.78, 0.39, 0.19, and 0.09 µM MG for one hour at 37°C, then the free MG was removed. Finally, ultrasound was performed on the cells at a frequency of 1 MHz with an intensity of 2 W/cm² and at a distance of 2 cm for 3 minutes.

Determination of in Vitro Efficacy of Sonodynamic Therapy

The experimental setup for MG-mediated SDT is shown in Figure 1. HL60 cells were centrifuged at 1000 rpm for 5 min after being exposed to various doses of MB for 1 h, as in our previous studies (19). PBS was added to the precipitate. This process was repeated 3 times, and then the free MG was removed. The BTL 4710 Sono dual-frequency ultrasound therapy device (BTL, CZ) was used to apply ultrasound to cells. Cells were transferred to 1.5 mL Eppendorf tubes and exposed to ultrasound at a frequency of 1 MHz, from a distance of 2 cm, and at an intensity of 2 W/cm² for 3 minutes (20) in water. To prevent the thermal effect of ultrasound, the water was changed, and the temperature of the application environment was kept under control. Subsequent to the ultrasound treatment, fresh medium was added to the samples, and the samples were incubated at 37°C for 24 hours.
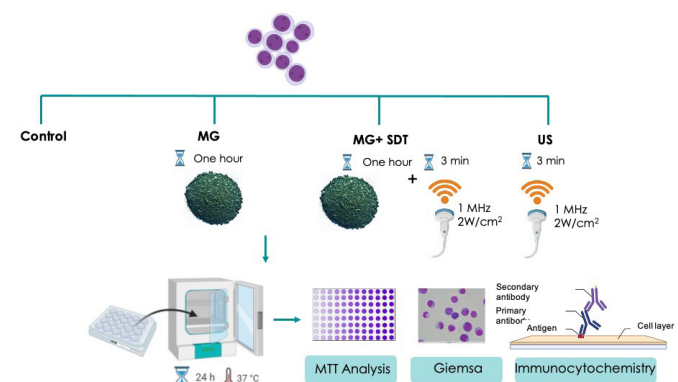

Figure 1. Experimental setup for MG-mediated SDT

MTT Analysis

Following the incubation period, cell viability was evaluated in the Control, US, MG, and MG mediated SDT groups using the MTT. The samples were incubated at 37°C and 5% CO_2 for 4 h using 10μl of MTT solution for each well in a 96-well microplate. Absorbance values were measured using a spectrophotometer at 570 nm (Multiskan Sky Microplate Spectrophotometer, Thermo Fisher Scientific).

Determination of Cell Morphology and Apoptotic Index Using Giemsa Staining

Three preparations were made for the control, US, MG, and MG mediated SDT groups. A certain amount of cells were taken from each group, spread on a slide, and allowed to dry. The dried cells were fixed by methanol. Giemsa stain, prepared in a one-to-one ratio with sterile distilled water, was dropped onto the slides with the preparations and left for 5 minutes. Subsequently, after washing off excess stain from the preparations, cell morphologies and apoptotic indices were examined under a light microscope. Cells containing condensed chromatin and micronuclei were considered apoptotic. The apoptotic index was determined by counting 100 cells in each group preparation, both apoptotic and non-apoptotic, at a magnification of 1000X.

Determination of ER Stress Markers GRP78 and PERK by Immunostaining

After centrifugation, the supernatant was removed, and the resulting precipitate was evenly distributed onto a slide. After the preparation dried, it was fixed with methanol. After PBS washing, it was incubated in a 3% H_2O_2 solution for 10 minutes to inhibit endogenous peroxidase activity. After washing with PBS again, normal goat serum (Invitrogen-50062Z) was applied for inhibition and left for 8 minutes. It was then incubated overnight with primary antibodies at +4°C: Anti-GRP78 BiP/HSPA5 (1:100, PB9640; Boster) and Anti-PERK (1:100, bs2469R; Bioss). After the incubation period, a rabbit anti-IgG secondary antibody (1/200, Thermo Scientific, 65-6140) was added to the preparations, and it was incubated for 30 minutes. Subsequently, the preparations were washed with PBS.

Horseradish peroxidase (HRP, 1/200, Thermo Scientific, 43-4323) was then added and incubated for 10 min. The reaction was further enhanced using the chromogen diaminobenzidine (DAB, Abcam, ab64238). After washing the preparations with distilled water, they were covered with Entellan and examined under a light microscope (Olympus BX50). Images were recorded using the attached camera. Immunocytochemical scoring was conducted by counting 100 cells in four different fields at 400X magnification. The staining intensities of these cells were scored as follows: strong (++++), moderate (+++), weak (+), and absent (+). The staining intensity score generally consists of four categories: negative (1), weak (2), moderate (3), and strong (4). The H-score, All red-score, and Immunoreactive score are regarded as the 'gold standard' in combined scoring

systems for evaluating and presenting IHC data. These scoring systems employ different categories to assess the proportion of stained tissues or cells (21).

Statistical Analysis

All experiments were repeated at least three times in triplicate wells. The data were analyzed using the SPSS 25.0 software, and one-way analysis of variance (ANOVA) and Paired Sample t-test were employed for data analysis. Results with a p-value <0.05 were considered statistically significant.

RESULTS

Effect of Malachite Green and Malachite Green-Mediated SDT on HL-60 Cell Viability

The results showed that SDT significantly reduced cell viability at all concentrations of MG compared to the control group, and cell death increased as concentrations of MG increased ($p<0.001$). Cell viability percentages of the Control, US, and MG mediated SDT groups, from low to high concentration, respectively, were determined as 99.7%±0.5, 97.5%±1.35, 95.6%±4.47, 94.4%±0.86, 86.6%±0.48, 75.6%±0.47, 52.3%±1.05, and 43.9%±2.28. No significant difference was observed between the control and US groups in terms of cell viability ($p>0.05$). In the MG group, cell viability percentages were determined as 98.2%±1.7, 99%±0.41, 99.95%±0.95, 97.7%±0.47, 88.6%±0.47 and 72.5%±1.15, respectively, from low concentration to high. It was observed that concentrations lower than 1.56 μM of MG did not significantly affect the viability of HL60 cells, while a concentration of 1.56 μM MG did have a small impact on viability and resulted in the death of approximately half of the cells when combined with US (Figure 2).
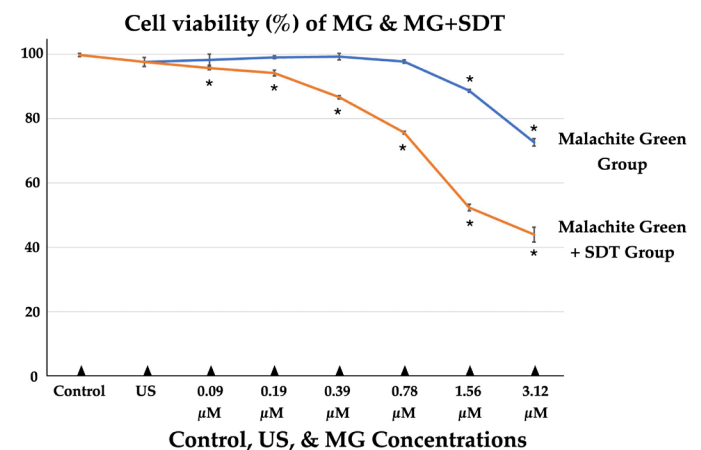

Figure 2. Evaluation of cytotoxicity after treatment with Control, Ultrasound, MG and MG-mediated SDT. The data represent the means±standard deviations (SDs) of 3 independent experiments. * indicates statistically significance compared to control group; Error bars 95% confidence interval

Determination of the Morphology and Apoptotic Index of HL60 Cells using Giemsa Staining

Morphological changes in cells are crucial for the determination of cell apoptosis. Figure 3A-G shows the

morphological findings of the control group and the MG treatment group at various concentrations. Typical morphological characteristics of HL60 cells in the control group were observed as large, round-nucleated, and cytoplasmic (Figure 3G). An increase in apoptotic cells with micronuclei was observed in the MG-only treated groups towards low to high concentrations (Figure 3A-F).

Figure 3I-O presents microscopic images of cells treated with US and MG-mediated SDT, after Giemsa staining. MG-mediated SDT groups showed irregular changes in morphology, including cell membrane shrinkage. It was observed that the number of apoptotic cells increased significantly as the MG concentration increased, and more apoptotic bodies were formed compared to the control. Apoptotic cells with irregular cytoplasmic contours, chromatin condensation, decreased nucleocytoplasmic ratio , and micronuclei were identified, particularly at high concentrations (Figure 3I-N). In the US-only group, typical morphological features were observed, although a few cells showed apoptotic cells with micronuclei (Figure 3O).

Apoptotic index values at the end of the 24-hour experimental period were calculated as 2.11±1.05% for the control group, 5.77±0.66% for the US group, 63.11±1.16%, 40.88±0.6%, 32.11±0.92%, 24.88±0.78%, 16.88±1.36%, and 8.22±1.31% for the 3.125 μM, 1.56 μM, 0.78 μM, 0.39 μM, 0.19 μM, and 0.09 μM MG-treated experimental groups, respectively, and 72.11±1.16%, 50.88±0.78%, 42.55±1.13%, 37.66±0.7%, 29.11±1.16%, and 11.88±0.78% for the MG+SDT group in the same MG concentration order (Figure 4).
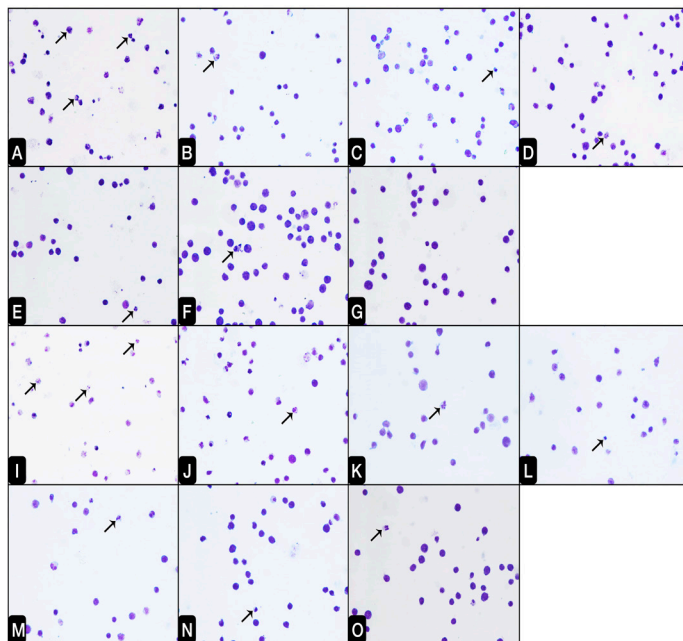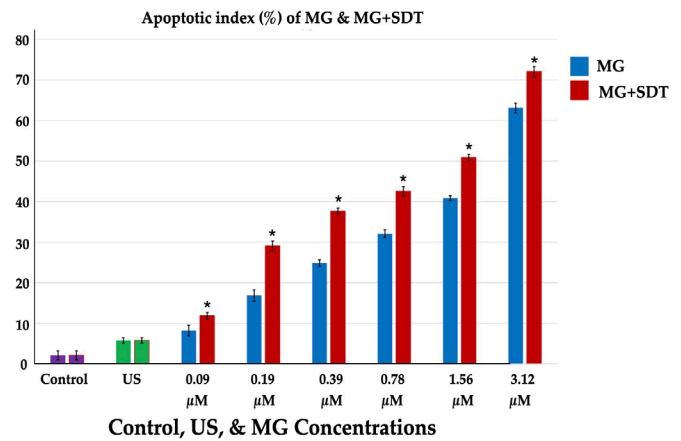

Figure 4. Apoptosis indices of control, US, MG and MG SDT groups.The data represent the means±standard deviations (SDs) of 3 independent experiments. *indicates statistically significance compared to control group; Error bars 95% confidence interval

Determination of ER Stress Markers GRP78 and PERK Expressions by Immunocytochemistry

GRP78 and PERK expressions in all groups were analyzed by examining the changes in immunocytochemistry staining. Compared to the control group, significant levels of GRP78 and PERK expression were observed in all groups (p<0.001) (Figure 5-7), except for PERK expression in the US group (Figure 6G). The expression of both proteins increased in both the MG group (Figure 5A-F and Figure 6A-F) and the MG-mediated SDT group (Figure 5I-N and Figure 6I-N) as the MG concentration increased.
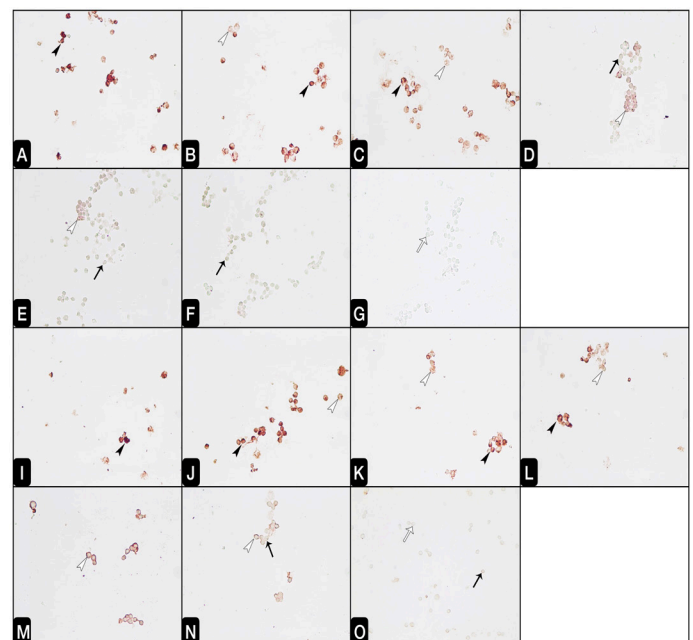

Figure 5. GRP78 immunostaining of MG and MG mediated SDT groups. 3.12 μM MG (**5A**), 1.56 μM MG (**5B**), 0.78 μM MG (**5C**), 0.39 μM MG (**5D**), 0.19 μM MG (**5E**), 0.09 μM MG (**5F**), Control (**5G**). 3.12 μM MG mediated SDT (**5I**), 1.56 μM MG mediated SDT (**5J**), 0.78 μM MG mediated SDT (**5K**), 0.39 μM MG mediated SDT (**5L**), 0.19 μM MG mediated SDT (**5M**), 0.09 μM MG mediated SDT (**5N**), US-Control (**5O**). Strong staining (black arrowhead), medium staining (white arrowhead), weak staining (black arrow), absent staining (white arrow). All photos imagination X400

Figure 3. Morphology of the MG and MG mediated SDT group: 3.12 μM MG (**3A**), 1.56 μM MG (**3B**), 0.78 μM MG (**3C**), 0.39 μM MG (**3D**), 0.19 μM MG (**3E**), 0.09 μM MG (**3F**), Control (**3G**), 3.12 μM MG mediated SDT (**3I**), 1.56 μM MG mediated SDT (**3J**), 0.78 μM MG mediated SDT (**3K**), 0.39 μM MG mediated SDT (**3L**), 0.19 μM MG mediated SDT (**3M**), 0.09 μM MG mediated SDT (**3N**), US-Control (**3O**) Apoptotic cells with micronuclei (black arrow). Magnification X400

Figure 6. PERK immunostaining of MG and MG mediated SDT groups. 3.12 μM MG (**6A**), 1.56 μM MG (**6B**), 0.78 μM MG (**6C**), 0.39 μM MG (**6D**), 0.19 μM MG (**6E**), 0.09 μM MG (**6F**), US (**6G**). 3.12 μM MG mediated SDT (**6I**), 1.56 μM MG mediated SDT (**6J**), 0.78 μM MG mediated SDT (**6K**), 0.39 μM MG mediated SDT (**6L**), 0.19 μM MG mediated SDT (**6M**), 0.09 μM MG mediated SDT (**6N**), US-Control (**6O**). Strong staining (black arrowhead), medium staining (white arrowhead), weak staining (black arrow), absent staining (white arrow). All photos imagination X400
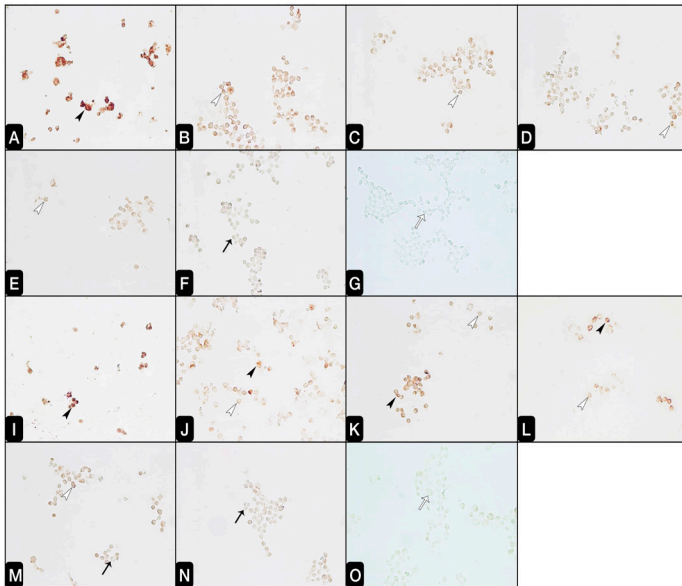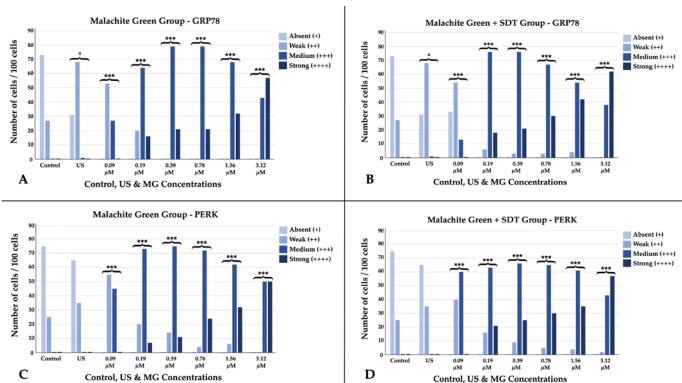

Figure 7. Statistical analysis of GRP78 MG Group (**7A**), GRP78 MG mediated SDT Group (**7B**), Statistical analysis of PERK MG groups (**7C**), PERK MG mediated SDT Group (**7D**). *** & °Significance according to the control groups

DISCUSSION

The combination of sensitizers and ultrasound has been reported to decrease cell viability and induce apoptosis in numerous studies in the literature. Li et al. reported that PpIX-mediated ultrasound treatment in the human leukemia cell line U937 significantly decreased cell viability, caused severe damage in cell morphology, DNA, and mitochondria. Furthermore, they noted that intracellular ROS were also involved in this process (22). In another study, Li et al. demonstrated that Ce6-mediated SDT suppressed the growth of K562 cells, increased intracellular ROS production, and triggered mitochondria and caspase-dependent apoptosis (23). Yumita et al. reported that the ATX-70 sonosensitizer does not cause cell damage when administered alone on HL60 cells, whereas cell damage occurred when activated with ultrasound (24). They showed in another study that apoptosis was induced by cell shrinkage, DNA fragmentation, and caspase 3 activation following fullerene-mediated SDT in HL60 cells (25). In their study on HL60 cells, Su et al. reported that protoporphyrin IX-mediated SDT increased the cytotoxicity of cells, HL-60 cell apoptosis was significantly induced, and intracellular ROS production increased significantly after SDT (26). In another study on U937 cells, they showed that Ce6-mediated SDT decreased cell viability, whereas treatment with Ce6 and US-only did not have an effect on cell viability, and that U937 cell apoptosis significantly increased after Ce6-mediated SDT (27). Trendowski et al. hypothesized that Cytochalasin B, a cytokinesis inhibitor that selectively enlarges and multinucleates malignant cells in U937 cells, may have significant therapeutic potential when combined with SDT (28).

According to our morphological results, the morphological features observed in the groups subjected to MG-mediated SDT include chromatin condensation, apoptotic cells with micronuclei, and cell shrinkage. Although a few cells with micronucleated apoptotic features were observed in groups treated only with MG and US, typical morphological characteristics were evident. These findings were consistent with apoptotic index results. In groups subjected to MG-mediated SDT, the apoptotic index ratio was found to be higher compared to the control, US, and MG-only groups.

Our results indicate that MG caused a significant decrease in cell viability starting at a concentration of 1.56 uM. However, when combined with ultrasound at this concentration, it resulted in the death of approximately half of the cells. At concentrations equal to or below this concentration, SDT is expected to have a beneficial effect. We observed that ultrasound alone did not affect cell viability, yet it caused a significant increase in GRP78 expression. We suggest that GRP78 (15), which plays a crucial role in the initial response to the increase in unfolded proteins and the triggering of the UPR, increases its expression in response to ultrasound-induced stress, This stress is tolerated by the cell without causing cell death, and viability remains unaffected. We conclude that PERK expression increases at advanced stages when ER stress becomes excessive, and naturally, no significant change occurs in its expression when exposed to the tolerable stress caused by ultrasound treatment.

CONCLUSION

All of our results indicate that MG-mediated SDT has a significant cytotoxic effect on cancer cells, accompanied or caused by significant ER stress when administered at the appropriate concentration. Further studies to elucidate the molecular mechanisms underlying this effect would contribute to the establishment of targeted therapies and the development of this alternative treatment more effectively. Our future perspective is to focus on the potential molecular mechanisms of this treatment and to investigate its similar or superior effects in other types of cancer.

Financial disclosures: *The authors declared that this study has received no financial support.*

Conflict of interest: *The authors have no conflicts of interest to declare.*

Ethical approval: *Since the methodological structure of the study is a "cell culture study", it does not require ethics committee approval in accordance with the World Medical Association Declaration of Helsinki "Ethical Principles for Medical Research on Humans".*

REFERENCES

1. Miller KD, Nogueira L, Devasia T, et al. Cancer treatment and survivorship statistics. Cancer J Clin. 2022;72:409-36.

2. Zou L, Wang H, He B, et al. Current approaches of photothermal therapy in treating cancer metastasis with nanotherapeutics.Theranostics. 2016;6:762-72.

3. Correia JH, Rodrigues JA, Pimenta S, et al Photodynamic therapy review: principles, photosensitizers, applications, and future directions. Pharmaceutics. 2021;13:1332.

4. Qian X, Zheng Y, Chen Y. Micro/nanoparticle-augmented sonodynamic therapy (SDT): breaking the depth shallow of photoactivation. Adv Mater. 2016;28:8097-129.

5. Yumita N, Nishigaki R, Umemura K, Umemura S. Hematoporphyrin as a sensitizer of cell-damaging effect of ultrasound. Jpn J Cancer Res.1989;80:219-22.

6. Gong F, Cheng L, Yang N, et al. Ultrasmall oxygen-deficient bimetallic oxide $MnWO_x$ nanoparticles for depletion of endogenous GSH and enhanced sonodynamic cancer therapy. Adv Mater. 2019;31:1900730.

7. Son S, Kim JH, Wang X, et al. Multifunctional sonosensitizers in sonodynamic cancer therapy. Chem Soc Rev. 2020;49:3244-61.

8. Chen H, Zhou X, Gao Y, et al. Recent progress in development of new sonosensitizers for sonodynamic cancer therapy. Drug DiscovToday. 2014;19:502-9.

9. Yu J, Guo Z, Yan J, et al. Gastric acid-responsive ROS nanogenerators for effective treatment of helicobacter pylori infection without disrupting homeostasis of intestinal flora. Adv Sci.2023;10:e2206957.

10. Liang S, Deng X, Ma PA, et al. Recent advances in nanomaterial-assisted combinational sonodynamic cancer therapy. Adv Mater. 2020;32:e2003214.

11. Canavese G, Ancona A, Racca L, et al. Nanoparticle-assisted ultrasound: A special focus on sonodynamic therapy against cancer. Chem Eng J. 2018;340:155-72.

12. Araki K, Nagata K. Protein folding and quality control in the ER. Cold Spring Harb Perspect Biol. 2011;3:a007526. Erratum in: Cold Spring Harb Perspect Biol. 2012;4:a015438.

13. Li D, Li L, Li P, et al. Apoptosis of HeLa cells induced by a new targeting photosensitizer-based PDT via a mitochondrial pathway and ER stress. Onco Targets Ther. 2015;8:703-11.

14. Lin S, Yang L, Shi H, et al. Endoplasmic reticulum-targeting photosensitizer Hypericin confers chemo-sensitization towards oxaliplatin through inducing pro-death autophagy. Int J Biochem Cell Biol. 2017;87:54-68.

15. Firczuk M, Gabrysiak M, Barankiewicz J, et al. GRP78-targeting subtilase cytotoxin sensitizes cancer cells to photodynamic therapy. Cell Death Dis. 2013;4:e741.

16. Ron D, Walter P. Signal integration in the endoplasmic reticulum unfolded protein response. Nat Rev Mol Cell Biol. 2007;8:519-29.

17. Sun XF, Wang SG, Liu XW, et al. Biosorption of malachite green from aqueous solutions onto aerobic granules: kinetic on equilibrium studies. Bioresour Technol. 2008;99:3475-83.

18. Montes de Oca MN, Vara J, Milla L, et al. Physicochemical properties and photodynamic activity of novel derivatives of triarylmethane and thiazine. Arch Pharm (Weinheim). 2013;346:255-65.

19. Caliskan-Ozlem S, Duran ÖF, Aslan C, et al. Therapeutic efficacy of malachite green-based photodynamic therapy in acute myeloid leukemia. J Contemp Med. 2023;13:305-11.

20. Yumita N, Iwase Y, Nishi K, et al. Involvement of reactive oxygen species in sonodynamically induced apoptosis using a novel porphyrin derivative. Theranostic. 2012;2:880-8.

21. Cizkova K, Foltynkova T, Gachechiladze M, et al. Comparative analysis of immunohistochemical staining intensity determined by light microscopy, Image J and QuPath in placental hofbauer cells. Acta Histochem Cytochem. 2021;54:21-9.

22. Li Y, Su X, Wang X, et al. Cytotoxic effect of protoporphyrin IX to human leukemia U937 cells under ultrasonic irradiation. Cell Physiol Biochem. 2014;33:1186-96.

23. Li Y, Wang P, Wang X, et al. Involvement of mitochondrial and reactive oxygen species in the sonodynamic toxicity of chlorin e6 in human leukemia K562 cells. Ultrasound Med Biol. 2014;40:990-1000.

24. Yumita N, Okudaira K, Momose Y, Umemura S. Sonodynamically induced apoptosis and active oxygen generation by gallium-porphyrin complex, ATX-70. Cancer Chemother Pharmacol. 2010;66:1071-8.

25. Yumita N, Watanabe T, Chen FS, et al. Induction of apoptosis by functionalized fullerene-based sonodynamic therapy in HL-60 cells. Anticancer Res. 2016;36:2665-74.

26. Su X, Wang X, Zhang K, et al. Sonodynamic therapy induces apoptosis of human leukemia HL-60 cells in the presence of protoporphyrin IX. Gen Physiol Biophys. 2016;35:155-64.

27. Su X, Wang P, Wang X, et al. Involvement of MAPK activation and ROS generation in human leukemia U937 cells undergoing apoptosis in response to sonodynamic therapy. Int J Radiat Biol. 2013;89:915-27.

28. Trendowski M, Yu G, Wong V, et al. The real deal: using cytochalasin B in sonodynamic therapy to preferentially damage leukemia cells. Anticancer Res. 2014;34:2195-202.